Atmos. Chem. Phys. Discuss., 10, 16861–16900, 2010
www.atmos-chem-phys-discuss.net/10/16861/2010/
doi:10.5194/acpd-10-16861-2010

Atmospheric Chemistry and Physics Discussions

Comparison between simulated and observed chemical composition of fine aerosols in Paris (France) during springtime: contribution of regional versus continental emissions

J. Sciare[1,*], O. d'Argouges[1], R. Sarda-Estève[1], C. Gaimoz[1], V. Gros[1], Q. J. Zhang[2], M. Beekmann[2], and O. Sanchez[3]

[1]LSCE, Laboratoire des Sciences du Climat et de l'Environnement, unité mixte CEA-CNRS-UVSQ, UMR8212, Gif-sur-Yvette, France
[2]LISA, Laboratoire Interuniversitaire des Sciences Atmosphériques, Université Paris Est and Paris 7, CNRS, Créteil, France
[3]AIRPARIF, Agence de Surveillance de la qualité de l'air, Paris, France

Received: 14 May 2010 – Accepted: 25 June 2010 – Published: 7 July 2010

Correspondence to: J. Sciare (jean.sciare@lsce.ipsl.fr)

Published by Copernicus Publications on behalf of the European Geosciences Union.

Abstract

Hourly concentrations of inorganic salts (ions) and carbonaceous material in fine aerosols (aerodynamic diameter, A.D.<2.5 µm) have been determined experimentally from fast measurements performed for a 3-week period in spring 2007 in Paris (France). The sum of these two chemical components (ions and carbonaceous aerosols) has shown to account for most of the fine aerosol mass ($PM_{2.5}$). This time-resolved dataset allowed investigating the factors controlling the levels of $PM_{2.5}$ in Paris and showed that polluted periods with $PM_{2.5}$ >15 µg/m^3 were characterized by air masses of continental (North-Western Europe) origin and chemical composition made by 75% of ions. By contrast, periods with clean marine air masses have shown the lowest $PM_{2.5}$ concentrations (typically of about 10 µg/m^3); carbonaceous aerosols contributing for most of this mass (typically 75%).

In order to better discriminate between regional and continental contributions to the observed chemical composition and concentrations of $PM_{2.5}$ over Paris, a comparative study was performed between this time-resolved dataset and the outputs of a chemistry transport model (CHIMERE), showing a relatively good capability of the model to reproduce the time-limited intense maxima observed in the field for $PM_{2.5}$ and ion species. Different model scenarios were then investigated switching off regional and European (North-Western and Central) emissions. Results of these scenarios have clearly shown that most of the ions observed over Paris during polluted periods, were either transported or formed in-situ from gas precursors transported from Northern Europe. By opposite, long-range transport from Europe appeared to poorly contribute to the levels of carbonaceous aerosols observed over Paris.

The model failed to properly account for the concentration levels and variability of secondary organic aerosols (SOA) determined experimentally by the EC-tracer method. The abundance of SOA (relatively to organic aerosol, OA) was as much as 75%, showing a poor dependence on air masses origin. Elevated SOA/OA ratios were also observed for air masses having residence time above ground for less than 10 h,

ACPD

10, 16861–16900, 2010

suggesting intense emissions and/or photochemical processes leading to rapid formation of secondary organic aerosols.

1 Introduction

Fine anthropogenic aerosols (with aerodynamic diameter, A.D., below 2.5 µm) have been recognized as having strong but poorly understood adverse effects on health (Nel, 2005); they may have also a significant climatic role at regional scales, inducing strong radiative forcing by directly scattering or absorbing sunlight and indirectly change cloud properties though the formation of cloud condensation nuclei (Ramanathan et al., 2007).

With more than half of the world population living in cities, urban areas represent nowadays one of the major sources of fine anthropogenic aerosols at global scale, pointing out the need for a better characterization of these aerosols in the neighboring of their emission sources. Atmospheric pollution and exposure levels in the densely populated megacities (cities having more than 10 million of inhabitants) will be particularly high since these cities are generally confined to a relatively small area; they can represent a major fraction of emissions of a given country (Gurjar et al., 2004).

With a population of about 12 millions inhabitants (20% of the French population), Greater Paris (France) is among the most populated megacity in Europe. Due to its favorable geographical situation (far from other big European cities and influenced very often by clean oceanic air masses), it may be considered as a good candidate for investigating the build-up of urban air pollution within temperate industrialized countries.

Particulate mass of fine aerosols ($PM_{2.5}$) is continuously monitored at several sites within Greater Paris since almost 8 years by the local air quality network (AIRPARIF), using a conventional on-line automatic system (R&P TEOM; see Patashnik and Rupprecht, 1991). During the period 2000–2006, levels of $PM_{2.5}$ in the region of Paris have shown rather stable yearly mean values ranging 13 to 16 µg/m^3 whereas primary pollutants monitored by AIRPARIF (carbon monoxide, sulfur dioxide, NO) have shown a net

ACPD
10, 16861–16900, 2010

decrease during this period (http://www.airparif.asso.fr). Since the year 2007, yearly mean concentration of $PM_{2.5}$ have substantially increased (up to 21 µg/m^3), partly due to the use of a new measurement technique (R&P TEOM-FDMS instrument) enabling a proper determination of the semi-volatile fraction of fine aerosols. Although this new method greatly improves the determination of $PM_{2.5}$, it has also brought $PM_{2.5}$ levels in the region of Paris closer to the 25 µg/m^3 yearly mean targeted value recommended by Europe for 2010 (limit value for 2015). Efficient abatement policies aiming at reducing levels of $PM_{2.5}$ in the region of Paris will have to be fed by preliminary $PM_{2.5}$ source apportionment studies and exhaustive aerosol chemistry studies (chemical mass balance) allowing a better separation between regional to continental aerosol sources.

Still few studies are available on the chemical speciation of aerosols in the Paris region. They comprise preliminary characterizations of carbonaceous aerosols (Ruellan and Cachier, 2001), carbon and lead isotopes (Widory et al., 2004) and semi-volatile species (Favez et al., 2007). Time-limited information in the chemical composition of fine aerosols in Paris have been recently reported by Gros et al. (2007) but for a site impacted by traffic which may not be fully representative for the composition and levels of aerosols in the Paris urban background atmosphere. Modelling studies over Paris have been reported in literature but concerned mainly PM with A.D.<10 µm (PM_{10}) or total suspended matter size fractions (Bessagnet et al., 2005; Hodzic et al., 2006). As a result, chemical composition of $PM_{2.5}$ over the region of Paris remains poorly documented and regional model simulating $PM_{2.5}$ concentrations and composition over this region poorly constrained.

In this context, time-resolved measurements of the major chemical constituents of fine aerosols may be particularly useful as they will offer a large database that can be used for model comparison. They may also help to better document large temporal variations in local emissions (such as traffic peaks generally observed at rush hours) as well as large diurnal fluctuation of the boundary height, thermodynamic equilibrium, ventilation, photochemistry, and air masses origin.

ACPD
10, 16861–16900, 2010

Hourly measurements of the main chemical constituents of $PM_{2.5}$ are reported here for the first time for the city of Paris and cover a 3-week period during spring 2007. Hourly reconstruction of $PM_{2.5}$ is calculated and compared with artifact-free $PM_{2.5}$ measurements obtained in parallel and independently. Regional and continental contributions to the major chemical constituents of $PM_{2.5}$ are discussed in light of this time-resolved dataset, backtrajectory air masses analysis, comparison with volatile organic compounds (VOC) dataset and comparison with the aerosol chemistry outputs of a regional chemistry transport model (CHIMERE) which is currently used for air pollution forecast by AIRPARIF and INERIS (www.prevair.org, Honoré et al., 2008).

2 Experimental

Atmospheric measurements were performed on the terraced roof (14m above ground level) of the Laboratoire d'Hygiène de la Ville de Paris (LHVP; Paris, 13th district; 48°44′44″ N, 2°21′35″ E). This site corresponds to a monitoring station of AIRPARIF and is considered as being representative of Paris background air pollution (Favez et al., 2007). Results presented here were obtained from 23 May 2007 to 10 June 2007. A wide variety of VOC has been measured during this campaign and is reported in details by Gros et al. (2010) and Gaimoz et al. (2010). Meteorological parameters were monitored at the site every 5min using a Campbell Scientific weather Station.

2.1 Field instruments

Artefact-free continuous (6-min time resolution) measurements of $PM_{2.5}$ (nonvolatile plus semi-volatile) were performed by a Tapered Element Oscillating Microbalance (TEOM) Model 1400 from Rupprecht and Pataschnik equipped with a Sample Equilibration System (SES) and a Filter Dynamic Measurement System (FDMS, 8500 model series) (Grover et al., 2005). This instrument delivers a concentration of semi-volatile material (SVM) in $PM_{2.5}$ which is mainly made of ammonium nitrate for Paris

ACPD
10, 16861–16900, 2010

background atmosphere (Favez et al., 2007). A very good agreement was found between our TEOM-FDMS measurements performed at LHVP (13th district) with similar performed by AIRPARIF in the center of Paris (1st district, les Halles), with $PM_{2.5}(LHVP) = 0.97 \times PM_{2.5}(Les\ Halles) + 0.19\ \mu g/m^3$; $r^2 = 0.95$; $N = 323$. This result indicates that our measurements are not significantly impacted by local contamination and may be representative for the Paris urban background atmosphere.

A mono-wavelength (525 nm) integrating nephelometer (ECOTECH, Model M9003) was operated in parallel with a 50% cut-off diameter inlet of 2.5 µm (sharp Cut cyclone Model SCC 1.828, BGI Incorp., MA) and provided light scattering coefficient (σ_{sp}) measurements every 5min. A silicagel Diffusion Dryer (Model 3062, TSI Incorp., USA) mounted upstream of the nephelometer was used to keep relative humidity (RH) inside the nephelometer below 30% in order to minimize the role of water uptake onto aerosols which is known to alter (σ_{sp}) measurements. More information on the operation, calibration, detection limit can be found in Sciare et al. (2008a).

Equivalent Black Carbon (EBC) measurements were obtained from 5-min integrated light absorption measurements performed by a seven-wavelength Aethalometer (Model AE-31, Magee Scientific) running at 5 LPM and equipped with a 50% cut-off diameter of 2.5 µm (R&P, Albany, NY).

Hourly concentrations of elemental carbon (EC) and organic carbon (OC) in $PM_{2.5}$ were obtained in the field from a semi-continuous ECOC field analyzer (Sunset Laboratory, Forest Grove, OR; Bae et al., 2004) running at 8 LPM. A denuder provided by the manufacturer was set upstream in order to remove possible adsorption of VOC onto the filter. Measurement uncertainty given by the ECOC analyzer is poorly described in literature and an estimate of 20% for this uncertainty was taken here following Peltier et al. (2007).

2.2 Filter sampling and chemical analyses

Fine (A.D.<2.5 µm) aerosols were collected continuously on 25-mm diameter pre-fired quartz filters (QMA) at a flowrate of 6.8±1.5 LPM and using the same sharp cut cyclone

ACPD
10, 16861–16900, 2010

as for the ECOC analyzer (Very Sharp Cut Cyclone (VSCC), BGI Inc., Waltham, MA). A denuder identical to the one used upstream of the ECOC analyzer was set between the cyclone and the filter holder in order to minimize artefacts due to VOC adsorption onto the filter matrix. Filter sampling interval was typically of the order of 12 h. A total of 36 filter samples were then collected during the campaign.

Half of the 25-mm diameter QMA filters were analyzed for their EC and OC content using a thermo-optical carbon analyzer (ECOC Lab Instrument, Sunset Lab.) implemented with the NIOSH thermal program (Birch and Cary, 1996). The uncertainty given by the manufacturer for EC and OC measurements is of 0.2 µgC/cm^2±5%. A total of 7 blanks were taken in the field covering the duration of the campaign and showed non detectable amounts of EC. An average value of 0.78±0.15 µgC/cm^2 for OC blanks was calculated and subtracted from the OC values obtained in the field.

Water-soluble organic carbon (WSOC) and ion analyses were achieved on the second half of the QMA quartz filters. WSOC measurements were performed using a total organic carbon analyzer (TOC, Model Sievers 900, Ionics Ltd, USA) in which ammonium persulphate and UV light (185 and 284 nm) are used for the oxidation and the quantification of organic carbon. Information on filter extraction protocol, detection limit, and calibration for WSOC analysis can be found in Sciare et al. (2008b). Concentrations of WSOC were corrected from blank filters taken in the field showing an average WSOC concentration of 0.54±0.18 µgC/cm^2. Ion composition (anions, cations) of the filter samples were also determined following the extraction and analytical protocol described in Sciare et al. (2005).

2.3 Validation of OC and EC field measurements

The consistency of our field measurements of EC and OC was checked by comparing results obtained by the ECOC field instrument, the aethalometer, and filter sampling. Hourly BC data obtained optically by the ECOC field instrument were compared with the equivalent BC data (EBC) given by the aethalometer when both instruments were running in parallel (23/05–10/06). A very good agreement was found between the 2

ACPD
10, 16861–16900, 2010

datasets ($r^2 = 0.94$; $N = 417$) with a slope close to one (0.96). Comparison between EC concentrations measured in the field (ECOC field instrument) with EC measurements obtained from filter sampling showed also a good agreement ($r^2 = 0.79$; $N = 34$) with a slope close to 1 (1.06). Similarly, comparison between OC concentrations measured in the field (ECOC field instrument) with OC measurements obtained from filter sampling showed a good agreement ($r^2 = 0.76$; $N = 34$) with a slope close to 1 (1.01). However, a significant intercept of 3.03 µgC/m^3 was found between these 2 datasets, pointing out a constant overestimation of OC concentration levels obtained in the field. Such an intercept has been reported in several studies (Arhami et al., 2006 ; Offenberg et al., 2007; Peltier et al., 2007) and could be due to filter artefacts in the ECOC field instrument. Field OC data discussed in the following were then corrected from this constant value of 3.03 µgC/m^3. Particulate organic matter (POM) concentrations reported in the following were calculated using an OC to POM conversion factor of 1.6 as proposed by Turpin and Lim (2001) for urban aerosols.

2.4 Determination of ion concentrations and reconstruction of $PM_{2.5}$

Hourly ion measurements were not available during this campaign but can be estimated using the reconstruction of the light scattering coefficient following the methodology reported in detail by Sciare et al. (2008a). Briefly, a simple model assuming an external mixing of the particles with constant dry mass scattering efficiencies and constant aerosol types (Malm et al., 1994, 2000) can be used here to reconstruct the light scattering coefficient (σ_{sp}), following the equation:

$$\sigma_{sp} = \alpha_{ions} f(RH)([(NH_4)_2SO_4] + [NH_4NO_3]) + \alpha_{POM}[POM] + \alpha_{seasalt}[seasalt] + \alpha_{dust}[dust] \quad (1)$$

Where α_X stands for the mass scattering efficiency of the chemical species $[X]$. It is assumed here that $(NH_4)_2SO_4$ and $(NH_4)NO_3$ have a similar mass scattering efficiency (α_{ions}) assigned to be 3 m^2/g, which is an average of values commonly reported in literature (Sciare et al., 2005 and references therein). The mass scattering efficiency of POM (α_{POM}) is taken equal to 4 m^2/g (Malm et al., 1994). Since nephelometer

ACPD
10, 16861–16900, 2010

measurements were poorly affected by water uptake onto aerosols, a constant enhancement factor, $f(\mathrm{RH})$, equal to 1 is taken here. The contribution of dust and sea salt aerosols to the light scattering coefficient (Eq. 1) is neglected here due to their low concentrations determined from filter sampling (data not shown here) and due to their low mass scattering efficiencies.

Based on these assumptions, Eq. (1) can be re-written as:

$$[\mathrm{ions}] = [(NH_4)_2SO_4] + [(NH_4)NO_3] = (\sigma_{sp} - 4 \times [\mathrm{POM}])/3) \quad (2)$$

Hourly concentrations of ions can be derived from this Eq. (2) for the whole period of measurement (23/05–10/06). An overall uncertainty associated with this ion calculation is estimated to be of the order of 30% (Sciare et al., 2008a) and takes into account uncertainties associated with the field instruments, OC-to-POM conversion factor, and light scattering efficiencies (α_{ions} and α_{POM}). Despite this important uncertainty, comparison of this ion dataset with filter data ion measurements (sum of ammonium, nitrate, sulfate) obtained in parallel and depicted in Sect. 2.2 shows very satisfactory results (slope of 1.03 and $r^2 = 0.76$; $N = 27$) and further validate the indirect method used here to calculate hourly concentration of ions (ammonium sulfate+ammonium nitrate).

These concentrations of ions were summed with concentrations of POM and EC (derived from the ECOC field instrument) in order to reconstruct $PM_{2.5}$ concentrations every hour. Comparison of this reconstructed $PM_{2.5}$ (noted as $PM_{2.5}$(CHEMISTRY)) with $PM_{2.5}$ concentrations obtained independently with the TEOM-FDMS monitor is reported in Fig. 1. A very good agreement can be observed here between these two datasets ($r^2 = 0.96$; $N = 418$) with a slope close to one (0.93) and an intercept close to zero ($-1.7\ \mu g/m^3$). This good accordance between measured and chemically reconstructed $PM_{2.5}$ demonstrates again the consistency of the hypotheses used to calculate hourly concentrations of ions and those to reconstruct $PM_{2.5}$ concentrations.

Finally, this result clearly shows that ions and carbonaceous aerosols can be considered as the two major components of Paris fine aerosols during springtime, in agreement with the study by Gros et al. (2007) who have reported that these chemical

ACPD
10, 16861–16900, 2010

species (ions and carbonaceous aerosols) contributed to almost 95% of the $PM_{2.5}$ in Paris during springtime.

3 Model description

The model used in this study is the Eulerian regional chemistry-transport model CHIMERE in its version V2008b (see http://euler.lmd.polytechnique.fr/chimere/). The initial gas phase chemistry scheme has been described by Schmidt et al. (2001) and Vautard et al. (2001), the aerosol modules by Bessagnet et al. (2004 and 2008). The model has been largely applied for continental scale air quality forecast (Honoré et al., 2008; http://www.prevair.org), and simulations, including sensitivity studies, with respect to biogenic emissions (Curci et al., 2009) and inverse emission modeling (Konovalov et al., 2006). The model has been also extensively used to simulate gas phase pollution levels over the Paris region (e.g., Vautard et al., 2001; Beekmann et al., 2003; Derognat et al., 2003; Deguillaume et al., 2007 and 2008), and on several occasions particulate matter (e.g. Bessagnet, 2005; Hodzic et al., 2006).

In this work, the model is set up on three successively nested grids: a continental domain (35–57.5° N; 10.5° W–22.5° E) with 0.5° resolution, a regional domain covering Northern France with 9 km resolution and a more refined regional/urban domain covering Ile-de-France region with a 3 km horizontal resolution (Fig. 2). In the vertical, eight hybrid-sigma vertical layers extend up to 500 hPa, the first layer extends up to about 40 m.

Tropospheric photochemistry is represented using the MELCHIOR chemical mechanism (Lattuati, 1997) that includes 120 reactions and 44 prognostic gaseous species. All major aerosol components are considered, namely primary organic (POA) and black (BC) carbon, other unspecified primary anthropogenic components, wind-blown dust, sea salt, secondary inorganics (sulfate, nitrate and ammonium) as well as secondary organic aerosols from anthropogenic and biogenic origin, and particulate water. A sectional size distribution over 8 size bins geometrically spaced from 40 nm to 10 µm in

ACPD
10, 16861–16900, 2010

physical diameter is chosen. The thermodynamic partitioning of the inorganic mixture (i.e. sulfate, nitrate, and ammonium) is computed using the ISORROPIA model (Nenes et al., 1998). Partitioning of semi-volatile VOC of anthropogenic and biogenic origin is governed by a "two product" SOA formation scheme (Pun and Seigneur, 2006), adapted by Bessagnet et al. (2008). The dynamical processes influencing aerosol growth such as nucleation, coagulation and absorption of semi-volatile species are included in the model as described by Bessagnet et al. (2004). Heterogeneous chemical processes onto particles and a simplified sulfur aqueous chemistry are also considered. Dry and wet deposition for all gaseous and aerosol species are computed as a function of the friction velocities and stability of the lowest model layer (Wesely, 1988), and as a function of grid-averaged precipitation rates and cloud water content (Tsyro, 2002). Clear sky photolysis rates are calculated off-line based on the TUV model (Madronich et al., 1998), and they are modified when in the presence of clouds. The numerical method for the temporal solution of the stiff system of partial differential equations is adapted from the second order TWOSTEP algorithm originally proposed by Verwer (1994), and is set-up using a time step of 2.5 min for chemistry.

Meteorological input is provided by PSU/NCAR MM5 model (Dudhia, 1993) run with three nested grids at 45 km (European domain), 15 km (North-West Europe and 5 km (Central France) resolution. In the vertical, 23 sigma layers extend up to 100 hPa. Meteorological fields are interpolated on the nested CHIMERE with horizontal and vertical resolution given above (Valari and Menut, 2008). MM5 is forced by the NCEP FNL (Final) Operational Global Analysis data from the Global Forecast System (GFS) operated four times a day in near-real time by the American National Centers for Environmental Prediction (NCEP), using the grid nudging (grid FDDA) option implemented within MM5. Anthropogenic gaseous and particulate emissions are derived from EMEP annual totals (http://www.ceip.at/emission-data-webdab/) and scaled to hourly emissions applying temporal profiles provided by IER (Friedrich, 1997). For the nested Northern France and Ile-de-France grid, refined emissions have been elaborated by the 6 ESMERALDA project partners that are, AIRPARIF, AIR NORMAND, ATMO PICARDIE,

ACPD
10, 16861–16900, 2010

ATMO CHAMPAGNE-ARDENNE, ATMO NORD PAS-DE-CALAIS and LIG'AIR. For gas phase species, they stem from a specific cadastre for Ile-de-France and Northern France (Elaboration of an inter-regional emissions inventory for the modeling platform of cartographic previsions ESMERALDA – 2005). For particulate matter emissions, a downscaling algorithm based on CORINE land-use data starting from EMEP annual totals is used to obtain spatially refined data. Splitting of $PM_{2.5}$ emissions is performed using the emission inventory of Laboratoire d'Aérologie (Junker and Liousse, 2008). Biogenic emissions are provided by the MEGAN data base (Guenther et al., 2006). LMDz-INCA monthly mean concentrations are used as boundary conditions (Hauglustaine et al., 2004).

4 Results and discussion of experimental data

A brief description of the temporal variations of $PM_{2.5}$, ion species, and carbonaceous aerosols is presented here. Back trajectories calculated for air masses observed during the field experiment are used to interpret the high variability in the concentration levels of $PM_{2.5}$ and ion species. Based on this analysis, contribution of regional/continental emissions are then discussed and confirmed from complementary VOC measurements, as well as from $PM_{2.5}$ measurements performed in the neighboring regions of Paris.

4.1 Temporal variation of the major chemical constituents of fine aerosols

Hourly concentrations of $PM_{2.5}$ (TEOM-FDMS), ions (sum of ammonium nitrate and ammonium sulfate calculated as described in the previous section) and carbonaceous aerosols (EC+POM) are reported in Fig. 3 for the 3-week duration of the campaign. An average $PM_{2.5}$ concentration of 24.3 $\mu g/m^3$ was calculated for this campaign which is close to the yearly (2007) $PM_{2.5}$ concentration of 21 $\mu g/m^3$ calculated for the urban area of Paris and illustrates that this campaign did not undergo unusual high levels of

ACPD
10, 16861–16900, 2010

$PM_{2.5}$ compared to the rest of the year.

Based on the time series of $PM_{2.5}$ concentration levels, this campaign could be divided into 3 distinct periods (noted I, II, and III in Fig. 3). The first and third periods were characterized by a strong variability in $PM_{2.5}$, with concentrations ranging from 5 to almost 70 µg/m^3, with intense but time-limited peak values and mean concentrations higher than the 25 µg/m^3 EU recommended limit value. The second period showed more stable concentrations of $PM_{2.5}$ with values around 10 µg/m^3. Interestingly, all the sharp maxima observed in $PM_{2.5}$ (Fig. 3) were related entirely with similar maxima in ions with concentration levels up to 50 µg/m^3. This strong covariation observed between $PM_{2.5}$ and ions observed is illustrated by the high correlation coefficient calculated between these 2 fractions ($r^2 = 0.93$). During the periods I and III, ions contributed to almost 75% of the fine aerosol mass. Although discrimination between ammonium nitrate and ammonium sulfate was not possible during our study, the role of ammonium nitrate could be partially inferred from the levels of semi-volatile material (SVM) measured by the TEOM-FDMS which show their highest values (typically ranging from 5 to 15 µg/m^3) during the periods with $PM_{2.5}$ >40 µg/m^3. By comparison, the contribution of SVM was typically less than 5 µg/m^3 for the period II.

It is interesting to note here that the variability of carbonaceous aerosols is completely disconnected to that of species with rather stable levels during the campaign, ranging from 5 to 10 µg/m^3. Their contribution to $PM_{2.5}$ is particularly weak during the episodes with $PM_{2.5}$ higher than 25 µg/m^3. On the other hand, they represent as much as 75% of $PM_{2.5}$ during the period II, characterized by low levels of $PM_{2.5}$ (and ions).

4.2 Backtrajectory analysis

In order to better characterize the periods I, II, and III, depicted previously in Fig. 3, 4-day back trajectories were calculated using the Hysplit Dispersion Model (Hybrid Single – Particle Lagrangian Integrated Trajectory; Draxler and Rolph, 2003; Rolph, 2003) with a 500 m height end point located at the sampling site. According to air masses origin,

ACPD
10, 16861–16900, 2010

the field campaign could be divided into the 3 distinct periods noted previously in Fig. 3 and displayed in Fig. 4. The first period of the campaign (4 days: 23 November 00:00–27 November 00:00 LT) was characterized by a high pressure system associated with air masses moving slowly and originating from Northern-Western Europe (Rhine-Ruhr region). During this period residence time of air masses above continental areas was typically of 72 h or more. The second period (7 days: 27 November 00:00–2 June 00:00 LT) was characterized by the presence of frontal (low pressure) systems and moderate western winds originating mainly from the Atlantic Ocean. During this period, residence time of air masses above the continental surface was less than 10 h. Air masses origin observed during the third period (9 days: 2 June 00:00–10 June 12:00 LT) was quite different and showed a pronounced North Eastern European influence. Residence time of these air masses above ground was again typically more than 72 h for this last period.

4.3 Regional and continental origin of the major chemical components of $PM_{2.5}$

The first period of the study (noted I in Fig. 3) is characterized by $PM_{2.5}$ ranging from 15 to 65 µg/m^3 and corresponds to continental air masses from North-Western Europe. The second period (noted II in Fig. 3) shows $PM_{2.5}$ typically below 10 µg/m^3 and corresponds to clean air masses from the Atlantic Ocean. Finally, the third and last period (noted III in Fig. 3) shows $PM_{2.5}$ typically ranging from 15 to 70 µg/m^3 and corresponds to continental air masses from North-Eastern Europe. Such air masses classification clearly shows that the highest levels of $PM_{2.5}$ (and ions) were observed during the periods with continental air mass advection.

In order to better infer regional versus continental contributions to $PM_{2.5}$ levels observed in Paris, the $PM_{2.5}$ concentration levels at 3 different sites, Paris – LHVP (this study), Bethune (suburban monitoring station from the ATMO PAS-DE-CALAIS air quality network), and St Jean (suburban monitoring station from the LIG'AIR air quality network) have been reported in Fig. 5. As displayed in this Figure, the temporal variation of $PM_{2.5}$ at these sites show common patterns, with a more pronounced contrast

ACPD
10, 16861–16900, 2010

between marine/continental air masses for the Paris-LHVP and St Jean stations. Interestingly, most of the sharp peaks observed in Paris are also seen at the other stations with a time lag of few hours suggesting large scale rather than local sources for these maxima of $PM_{2.5}$. Based on these results, it can reasonably be hypothesized that most of the ion species observed in Paris during our study were transported (or formed during their transport) from continental Europe and were spread over large areas. This hypothesis is consistent with the EMEP inventories which show large emission areas over North-Western Europe for the gas precursors (NH_3, NO_x, SO_2) of ion species. It is also consistent with the fact that ion production requires atmospheric ageing to occur and subsequently is expected to show higher values downwind of the emission sources of their gas precursors.

It is interesting to note here that the influence of air masses origin on ion concentration levels is also observed for oxygenated VOCs such as acetone and methanol which show much higher baseline levels in continentally influenced than in oceanic air (Gros et al., 2010) (data not shown here). Acetone has an intermediate lifetime of about one month with primary sources mainly of biogenic origin but has also an important contribution from secondary sources (namely oxidation of non methane hydrocarbon, NMHC). Such good accordance between ion species and oxygenated VOCs points the fact that both fractions are photochemically produced.

As shown in Fig. 3, the fact that carbonaceous aerosols are rather stable during this study (e.g. poorly dependent on air masses origin) suggests that the main sources of these particles may be regional (i.e. within the Greater Paris agglomeration). This is consistent with the diurnal variation of EC which shows its highest levels during rush hours (around 08:30 local time), independently of air mass origin. This is also in line with the results obtained from NMHC measurements performed in parallel showing a poor influence of air mass origin, and a major local/regional source (vehicle exhaust and fuel evaporation) (Gaimoz et al., 2010).

ACPD
10, 16861–16900, 2010

5 Model comparison and simulation of continental versus regional contributions

A preliminary interpretation of the temporal variability of experimental data ($PM_{2.5}$, ion species, and carbonaceous aerosols) has been proposed in the previous section and has shown that the maxima of $PM_{2.5}$ observed during our study were mainly due to ion species originating from North-Western Europe and spreading over large areas during their transport. Whether these ions have been transported from continental Europe or have been formed during their transport still remains unclear based on our present dataset.

Although these results suggest that long range transport may significantly contribute to the levels of ions in Paris, regional pollution build-up and its contribution to the levels of ions (and carbonaceous aerosols) cannot be ruled out. Changes in meteorological conditions (ventilation, boundary height, thermodynamic equilibrium) and photochemistry between marine and continental air masses may also significantly affect the levels and composition of $PM_{2.5}$ in a way that is hardly predictable using solely experimental dataset. The apparent poor contribution of European carbonaceous aerosols compared to regional emissions requires also more attention. Discrimination between primary and secondary organic aerosol may be needed here to better identify the origin of this carbonaceous matter.

In order to distinguish the regional from the continental contribution to $PM_{2.5}$ concentrations and chemical composition, a comprehensive chemical transport model (CHIMERE) is used and its results are compared with experimental data. A first qualitative approach of regional/continental influences is presented for 2 consecutive pollution events. Model outputs are then tested against observations for $PM_{2.5}$, ions, and carbonaceous aerosols (EC+POM). Different scenarios are investigated using CHIMERE, "switching" OFF consecutively the regional and continental sources of gas precursors of ions and carbonaceous aerosols. A last focus is made on carbonaceous aerosols; different experimental methods are used to discriminate between primary and sec-

ACPD
10, 16861–16900, 2010

ondary organic aerosols and are then compared with model outputs in order to depict their regional-to-continental contribution.

5.1 Plume case study

Two consecutive (partly overlapping) pollution events modeled by CHIMERE for the 4^{th} of June are displayed in Fig. 6; a first one for fine nitrate (3 June 20:00 LT–4 June 12:00 LT) and a second for fine sulfate (4 June 04:00 LT–5 June 01:00 LT).

The first episode (Fig. 6a) shows a nitrate plume progressing from Benelux to the Paris region. It corresponds to the period noted with a black star in Fig. 3). Inspection of gaseous precursor emission maps suggest that ammonium nitrate formation occurs as a result of strong NO_x emissions over the Rhine-Ruhr region oxidizing to HNO_3, and mixing with air masses having encountered strong ammonia emissions over the Netherlands and Belgium.

The second episode (Fig. 6b) occurs a day later and shows a burst in concentration of fine sulfate over a large area (Rhine-Rhur region, North of France, Central England) within few hours (4 June in the morning). Most of this burst of fine sulfate observed on the 4 June corresponds to an intense in-situ photochemical oxidation of SO_2. It should be noted that the region of Paris is located at the limit of the geographic zone where these two events occurred which may partly explain the time-limited duration of these episodes of fine nitrate and sulfate over this region (Fig. 3). Note also that these 2 events simulated by CHIMERE highlight the major role of gas precursors (NO_x, SO_2) and their potential to be transported and converted into fine nitrate and sulfate far from their emission sources.

5.2 Temporal variation of experimental and modelled fine aerosol constituents

Comparison between modelled and experimentally determined concentrations of $PM_{2.5}$, ions and carbonaceous matter is reported in Fig. 7. To our best knowledge, this is the first time that the CHIMERE model is tested against time-resolved (hourly)

ACPD
10, 16861–16900, 2010

experimental determination of ions and carbonaceous matter.

First, the general good agreement observed in this Figure for all the chemical constituents of fine aerosols demonstrates the capability of the model to account for most of their variability and concentrations observed in Paris. As previously reported from experimental data, the results of the model clearly show that all the temporal variability of $PM_{2.5}$ is due to a similar variability in ions. The poor temporal variability of carbonaceous matter is also properly reproduced by the model.

Few discrepancies are observed between experimental and modelled results and concern mainly a simulated - but not observed – peak of carbonaceous aerosols (25 May) and, second, a peak of ions observed for the period (8–10 June) not seen by the model. On 25 May, simulated carbonaceous aerosol is largely overestimated (as well as NO_x). This is due to an underestimated boundary layer height, simulated at below 200 m at 08:00 UTC, as compared to an observed one at about 500 m (from aerosol backscatter lidar measurements at the SIRTA site 20 km in SW of Paris centre, http://sirta.ipsl.polytechnique.fr/data-search/2.html). The peak of ions observationally determined for the period (8–10 June) and not reproduced by the model may originate from several reasons: a weak model capability to properly reproduce in time and space rain events which has been made evident for this episode by comparing simulated precipitation fields with observed ones (from rain radar), Errors in humidity and cloud water content could also affect ion formation. Last, part of ions appears in the coarse mode probably due to numerical diffusion in the coagulation scheme.

5.3 Model evaluation of the regional-to-continental contribution to $PM_{2.5}$ levels in Paris

In order to better distinguish between regional and continental pollution origin, two different domains were defined in the CHIMERE grid domain reported in Fig. 2: the first domain labelled “IDF” (standing for Ile-de-France region) comprising the region of Paris, the second region (labelled “EU”) comprising part of North-Western and Central Europe. Two different scenarios are then evaluated in the following, based on these 2

ACPD
10, 16861–16900, 2010

grid domains:

- A first scenario labelled “Impact of regional emissions” which is the difference between a reference run and a run with all anthropogenic and biogenic gas and particulate matter emissions from the Ile-de-France region removed.
- A second scenario labelled “Impact of EU emissions” is obtained from the difference between the reference run and a run in which all emissions from EU domain have been removed.

Fine nitrate and fine sulfate simulated with these different scenarios are reported in Fig. 8. Note that the sum of the red (impact of regional emissions) and grey lines (impact of EU emissions) can exceed the blue line (reference) in Fig. 8, due to non-additive effects (thermodynamic equilibrium, impact of emissions on OH).

Model scenarios for ion species: During the periods I and III, results from the model (Fig. 8) clearly show that most of the concentrations modelled for nitrate and sulfate can be explained by build-up from European emissions and advection to the Ile-de-France region. This result is illustrated by the similarity of the blue curve (reference) and the grey curve (impact from EU emissions). This result unambiguously shows the major contribution of EU emissions during the periods with high $PM_{2.5}$ concentration levels pointing out the need for larger scale abatement strategies aiming reducing $PM_{2.5}$ in the region of Paris.

Outputs of the model also suggest that nitrate is responsible for most of the sharp peaks observed for ions. Such variability likely originates from important changes in thermodynamic equilibrium responsible for the condensation/evaporation of nitrate. It may also originate from rapid formation as indicated by the model which calculates, for some days, local formation of nitrate and sulfate from rapid oxidation of regionally emitted NO_x and SO_2 (for the latter due to the presence of clouds).

Model scenarios for carbonaceous species: Results of the 2 scenarios (Impact of regional and EU emissions) for primary carbonaceous aerosols clearly point to a major

ACPD
10, 16861–16900, 2010

contribution of regional sources (data not shown here), which appears to be consistent with our previous observations.

In order to better characterize the role and the origin of secondary organic aerosols (SOA) in Paris, different experimental methods are used in the following to discriminate between primary and secondary organic aerosols and are then compared with model outputs in order to depict their regional and continental contribution.

5.4 Experimental evaluation of primary and secondary organic aerosols

Previous findings on carbonaceous aerosols (EC+POM) have suggested a dominant role of regional emissions for this fraction. However, this does not necessarily imply that all these particles are of primary origin. Figure 9 depicts normalized daily variations of EC, OC, and OC/EC ratio during the whole sampling period. These normalized data are obtained from normalized hourly data of EC, OC and EC/OC ratio calculated as hourly ratios divided by a 24 h mean ratio centered on each hourly ratio. This Fig. 9 shows EC maxima at rush hours (around 08:00 in the morning and 20:00 in the evening) which are consistent with dominant regional traffic emissions. In contrast, daily variations of OC do not follow this trend, showing 2 maxima (one in the afternoon, and one at the evening, during the rush hour period). The increase of OC in the afternoon is observed at the maximum of solar radiation and may correspond to a secondary production mechanism of organic aerosol, probably induced by photochemistry. Similar secondary production of organics have been already reported and discussed in detail for the Paris region during summer by Favez et al. (2007). The first maximum of the OC/EC ratio observed during the afternoon is then driven by a photochemical production of OC. The second maximum observed during nighttime for this ratio has been also observed during wintertime (Sciare et al., 2010) and may be due to a temperature driven condensation mechanism of semi-volatile species (Fan et al., 2004).

Two different methods are applied in the following to estimate experimentally the fraction of secondary organic aerosols. The first one is based on the use of WSOC as a proxy for oxygenated secondary organics (Weber et al., 2007; Kondo et al., 2007),

ACPD
10, 16861–16900, 2010

SOA corresponding to water soluble organic matter (WSOM). Primary organic aerosols (POA) are then assumed to correspond to water insoluble organic matter (WIOM). WSOM and WIOM are calculated here using WSOC and WIOC data from filter sampling. WSOC-to-WSOM and WIOC-to-WIOM conversion factors of 2.1 and 1.3, respectively, are taken here (Turpin and Lim, 2001; Zhang et al., 2005).

The EC-tracer method (Turpin and Huntzicker, 1991) can be used here as a second method to estimate SOA. This method is based on the use of a minimum in the OC/EC ratio which can be related to primary emissions and which is used to calculate POA; any increase of the OC/EC from this minimum being related to a secondary production of organic aerosols. One of the major issues of this method is related to the proper choice of OC/EC of primary origin. Our lowest OC/EC ratios (~0.7) were taken as the one characteristic for primary emissions. These ratios were observed at the morning peak of EC (traffic) and for air masses originating from the ocean (e.g. minimizing continental emissions). These ratios are in good agreement with those reported by Lonati et al. (2007) for measurements performed in tunnels. Primary organic carbon (POC) was calculated using the equation [POC]/[EC]=0.7. Secondary Organic Carbon (SOC) was then calculated as the difference between OC and POC. SOA and POA from the EC-tracer method were calculated using a SOC to SOA and POC to POA conversion factors of 2.1 and 1.3, respectively (Turpin and Lim, 2001; Zhang et al., 2005).

Comparison between POA and SOA calculated from these two different approaches is reported in Fig. 10 and shows comparable mean concentration levels (typically around 1–2 $\mu g/m^3$ for POA, and 3–5 $\mu g/m^3$ for SOA). On the other hand, POA and SOA temporal variabilities derived with these 2 methods are poorly correlated. A first explanation can be related to the validity of the water soluble properties of SOA since freshly formed water insoluble SOA has already been reported in urban atmosphere (Favez et al., 2008). Beyond this discrepancy, it remains interesting to note that SOA determined by the EC-tracer method is clearly influenced by air mass origin, the highest SOA levels being observed for the periods I and III with mean concentrations of 6.7±2.7 $\mu g/m^3$

ACPD
10, 16861–16900, 2010

and 3.6±1.5 µg/m^3, respectively. As for ion species, it is legitimate to assume that European emissions may have contributed to these high levels of SOA through high emissions of biogenic and anthropogenic gas precursors. Significant amounts of SOA (2.7±1.7 µg/m^3) are still determined for the second period which is characterized by marine air masses having residence time less than 10 h, suggesting here a non negligible formation of fresh SOA in the vicinity of the region of Paris. This is confirmed by the SOA/OA ratio which is poorly affected by air masses origin, showing average values of 79%, 73%, and 72% for the 3 consecutive periods, respectively. Such results clearly illustrate the strong potential to create rapidly significant amounts of SOA in the vicinity of the region of Paris.

5.5 Comparison between modelled and experimentally determined primary and secondary organic aerosols

Measured and modeled concentration of carbonaceous aerosols (EC+POM) has shown previously quite similar concentration levels (Fig. 7c). Detailed comparison of the different observed and simulated carbonaceous fractions (EC, POA, SOA) reported in Fig. 10 is much less satisfactory. Experimental and simulated EC are quite similar in concentration levels although they present a poor correlation coefficient ($r^2 = 0.52$). Modeled POA is a factor of two higher than the EC-tracer derived POA. This difference can be simply explained by the different methods used to calculate POA. As for the EC-tracer method, the model derives POA directly from EC concentrations using a ratio [POA]/[EC] of 1.35, which is almost a factor of 2 higher compared to the one we have taken for the EC-tracer method. By contrast, model derived SOA is a factor of two lower compared to the one estimated with the EC-tracer method.

As for a conclusion, the concordance between modeled and measured concentration of carbonaceous aerosols (EC+POM) observed in Fig. 7c, results from an overestimation (respectively underestimation) of POA (respectively SOA). In the model, EC and POA are clearly of regional origin, which is consistent with the disconnected variations

ACPD
10, 16861–16900, 2010

of carbonaceous aerosol and ions observed in experimental data. However, due to the underestimation of SOA, the model cannot be used at this stage to conclude on the regional/continental origin of experimentally derived SOA.

6 Conclusions

Time-resolved measurements of the chemical composition of fine aerosols were performed in Paris (France) during springtime and used to calculate hourly concentrations of ions (ammonium nitrate+ammonium sulfate) and carbonaceous aerosols (EC and POM) in $PM_{2.5}$. These two components have shown to be the main contributors to $PM_{2.5}$ in Paris, although these contributions appeared to be highly variable, ranging from 25 to 75%.

Periods with high levels of $PM_{2.5}$ (>10–15 µg/m^3) have shown to be associated with continental air masses regimes and were mainly composed of ions (ammonium nitrate and ammonium sulfate). Comparison of our $PM_{2.5}$ dataset with others obtained in the North of France during the same period has shown that these intense pollution episodes were not a local pattern of the region of Paris but a widely spread pollution originating from continental Europe. Comparison with VOC measurements performed in parallel has revealed a close relationship between ions and oxygenated VOCs (methanol, acetone) with higher concentrations during periods influenced by continental air masses. Both fractions being produced through photochemical processes, their apparent concordance suggested that Paris region was under the influence of continental photochemically aged air masses during the episodes with elevated $PM_{2.5}$ levels. In contrast with ion species, concentrations of carbonaceous aerosols observed during this study were more stable (poorly influenced by air masses origin), suggesting a more regional pattern for this fraction.

In order to determine regional and continental contributions to the concentration levels and composition of fine aerosols over the region of Paris, our time-resolved measurements were first compared with the results of a chemistry transport model

ACPD
10, 16861–16900, 2010

(CHIMERE) currently used by the local air quality network (AIRPARIF) for air pollution forecast. As a whole, this comparison appeared satisfactory, the model being able to predict almost every peak value observed in $PM_{2.5}$. Specifically, the model has shown to overestimate the local influence (primary carbonaceous aerosol) while underestimating SOA and continental advection of ions to the area.

Different scenarios were evaluated with this model, switching OFF regional and continental emissions, respectively. Results obtained for ions clearly showed a major EU contribution, in agreement with our previous observations. Also most of the sharp peak values observed for ions (and $PM_{2.5}$) were mainly due to semi-volatile nitrate originating from the Rhine-Ruhr region. Model results obtained for carbonaceous aerosols appeared to agree well with our previous observations suggesting an important contribution from regional emissions.

Although these results clearly need to be extended to the rest of the years, they suggest that EU emissions may play a significant role during the periods with high $PM_{2.5}$ levels over the region of Paris. This result is relevant for local policy makers which have to propose efficient abatement strategies aiming at reducing $PM_{2.5}$ concentration levels in the context of an EU limit value of 25 µg/m^3 in 2015. On the other hand, implications of our results for health issues are less evident since the $PM_{2.5}$ peak values of fine aerosols observed during our study were mainly composed of ions, which present a poor toxicity relative to the other trace elements in fine aerosols (metals, PAH, . . .).

Finally the regional/continental contribution to secondary organic aerosols measured over Paris has been investigated. Two different methods were used to experimentally estimate the secondary fraction of organic aerosols and showed that SOA were likely tp play a major role in Paris during springtime, representing about 75% of the total mass concentration of organic aerosols. As expected, periods influenced by photochemically processed continental air masses showed the highest concentrations of SOA. Surprisingly, our results suggest that the abundance of SOA (relatively to OA) did not exhibit significant changes between the periods influenced by clean marine and photochemically processed continental air masses, respectively. Although this work has provided

ACPD
10, 16861–16900, 2010

limited information on (S)OA, these results suggest that regional emissions may have been quite important and/or have reacted quite rapidly, bringing the relative abundance of SOA at similar levels compared to continental aged air masses. Comparison between modeled and measured primary (respectively secondary) organic aerosols has shown significant discrepancies with overestimation (respectively underestimation) by a factor of 2 for model calculation, pointing out the need for a better model evaluation of processes leading to SOA.

Acknowledgements. This work was supported by the Agence Nationale de la Recherche (ANR) through the AEROCOV project, ADEME, CNRS, and CEA. Authors want to acknowledge LHVP (A. Person, Y. Le Moullec) for having hosted this field experiment. Contribution of local air quality networks (AIRPARIF, LIGAIR, ATMO NORD PAS-DE-CALAIS, AIR NORMAND, ATMO CHAMPAGNE-ARDENNE, and ATMO PICARDIE) are also acknowledged here through the access of $PM_{2.5}$ data at Paris, Bethune, and St Jean and emission data. Modeling results have been obtained under Ph-D grant funding by CIFRE (ANRT) attributed to ARIA Technologies and LISA. The authors gratefully acknowledge the NOAA Air Resources Laboratory (ARL) for the provision of the HYSPLIT transport and dispersion model and/or READY website (http://www.arl.noaa.gov/ready.php) used in this publication..

The publication of this article is financed by CNRS-INSU.

References

Arhami, M., Kuhn, T., Fine, P. M., Delfino, R. J., and Sioutas, C.: Effects of sampling artifacts and operating parameters on the performance of a semicontinuous particulate elemental

ACPD
10, 16861–16900, 2010

carbon/organic carbon monitor, Environ. Sci. Technol., 40, 945–954, 2006.
Bae, M. S., Schauer, J. J., DeMinter, J. T., Turner, J. R., Smith, D., Cary, R. A.: Validation of a semi-continuous instrument for elemental carbon and organic carbon using a thermal-optical method, Atmos. Environ., 38, 2885–2893, 2004.
Beekmann, M. and Derognat, C.: Monte Carlo uncertainty analysis of a regional scale transport chemistry model constrained by Measurements from the Esquif campaign, J. Geophys. Res., 108, 8559, doi:10.1029/2003JD003391, 2003.
Bessagnet, B., Hodzic, A., Vautard, R., Beekmann, M., Cheinet, S., Honoré, C., Liousse, C., and Rouil, L.: Aerosol modelling with Chimere – Preliminary evaluation at the continental scale, Atmos. Environ., 38, 2803–2817, 2004.
Bessagnet, B., Hodzic, A., Blanchard, O., Lattuati, M., Le Bihan, O., Marfaing, H., and Rouil, L.: Origin of particulate matter pollution episodes in wintertime over the Paris basin, Atmos. Environ., 39, 6159–6174, 2005.
Bessagnet, B., Menut, L., Curci, G., Hodzic, A., Guillaume, B., Liousse, C., Moukhtar, S., Pun, B., Seigneur C., and Schulz, M.: Regional modeling of carbonaceous aerosols over Europe – focus on secondary organic aerosols, J. Atmos. Chem., 61, 175–202, 2008.
Birch, M. E. and Cary, R. A.: Elemental carbon-based method for monitoring occupational exposures to particulate diesel exhaust, Aer. Sci. and Technol., 25, 221–241, 1996.
Curci, G., Beekmann, M., Vautard, R., Smiatek, G., Steinbrecher, R., Theloke, J., and Friedrich, R.: Modelling study of the impact of isoprene and terpene biogenic emissions on European ozone levels, Atmos. Environ., 43, 1444–1455, 2009.
Derognat, D., Beekmann, M., Baeumle, M., Martin, D., and Schmidt, H.: Effect of biogenic VOC emissions on the tropospheric chemistry during elevated ozone periods in Ile de France, J. Geophys. Res., 108, 8560, doi:10.1029/2001JD001421, 2003.
Deguillaume, L., Beekmann, M., and Menut, L.: Bayesian Monte Carlo analysis applied to regional scale inverse emission modelling for reactive trace gases, J. Geophys. Res., 112, D02307, doi:10.1029/2006JD007518, 2007.
Deguillaume, L., Beekmann, M., and Derognat, C.: Uncertainty evaluation of ozone production and its sensitivity to emission changes over the Ile-de-France region during summer periods, J. Geophys. Res., 113, D02304, doi:10.1029/2007JD009081, 2008.
Draxler, R. R. and Rolph, G. D.: HYSPLIT (HYbrid Single-Particle Lagrangian Integrated Trajectory) Model access via NOAA ARL READY Website (http://www.arl.noaa.gov/HYSPLIT.php). NOAA Air Resources Laboratory, Silver Spring, MD, 2003.

ACPD
10, 16861–16900, 2010

Dudhia, J.: A nonhydrostatic version of the Penn State/ NCAR mesoscale model: validation tests and simulation of an Atlantic cyclone and cold front, Mon. Weather Rev., 121, 1493–1513, 1993.

Fan, X., Lee, P. K. H., Brook, J. R., and Mabury, S. A.: Improved measurement of seasonal and diurnal differences in the carbonaceous components of urban particulate matter using a denuder-based air sampler, Aer. Sci. Technol., 38, 63–69, 2004.

Favez, O., Cachier, H., Sciare, J., and Le Moullec, Y.: Characterization and contribution to $PM_{2.5}$ of semi-volatile aerosols in Paris (France), Atmos. Environ., 41, 7969–7976, 2007.

Favez, O., Sciare, J., Cachier, H., Alfaro, S. C., and Abdelwahab, M. M.: Significant formation of water-insoluble secondary organic aerosols in semi-arid urban environment, Geophys. Res. Lett., 35, L15801, doi:10.1029/2008GL034446, 2008.

Friedrich, R.: GENEMIS: assessment, improvement, temporal and spatial disaggregation of European emission data, in: Tropospheric Modelling and Emission Estimation, Part 2, edited by: Ebel, A., Friedrich, R., and Rhode, H., Springer, New York, 181–214, 1997.

Gaimoz, C., Sauvage, S., Gros, V., Herrmann, F., Williams, J., Locoge, N., Perrussel, O., Bonsang, B., d'Argouges, O., Sarda-Estève, R., and Sciare, J.: Volatile organic compounds sources in Paris in spring 2007. Part II: source apportionment using positive matrix factorization, Atmos. Environ., submitted, 2010.

Gros, V., Sciare, J., and Yu, T.: Air Quality Air-quality measurements in megacities: Focus on gaseous organic and particulate pollutants and comparison between two contrasted cities, Paris and Beijing, C. R. Geosci., 339, 764–774, 2007.

Gros, V., Gaimoz, C., Herrmann, F., Custer, T., Williams, J., Bonsang, B., Sauvage, S., Locoge, N., d'Argouges, O., Sarda-Estève, R., and Sciare, J.: Volatile organic compounds sources in Paris in spring 2007. Pat I: qualitative analysis, Atmos. Environ., submitted, 2010.

Grover, B. D., Kleinman, M., Eatough, N. L., Eatough, D. J., Hopke, P. K., Long, R. W., Wilson, W. E., Meyer, M. B., and Ambs, J. L.: Measurement of total $PM_{2.5}$ mass (nonvolatile plus semivolatile) with the Filter Dynamic Measurement System tapered element oscillating microbalance monitor, J. Geophys. Res., 110, D07S03, doi:10.1029/2004JD004995, 2005.

Guenther, A., Karl, T., Harley, P., Wiedinmyer, C., Palmer, P. I., and Geron, C.: Estimates of global terrestrial isoprene emissions using MEGAN (Model of Emissions of Gases and Aerosols from Nature), Atmos. Chem. Phys., 6, 3181–3210, doi:10.5194/acp-6-3181-2006, 2006.

Gurjar, B. R., Butler, T. M., Lawrence, M. G., and Lelieveld, J.: Evaluation of emissions and air

ACPD
10, 16861–16900, 2010

quality in megacities, Atmos. Environ., 42, 1593–1606, 2008.
Hauglustaine, D. A., Hourdin, F., Jourdain, L., Filiberti, M.-A., Walters, S., Lamarque, J.-F., and Holland, E. A.: Interactive chemistry in the Laboratoire de Météorologie Dynamique general circulation model: Description and background tropospheric chemistry evaluation,J. Geophys. Res., 109, D04314, doi:10.1029/2003JD003957, 2004.
Hodzic, A., Vautard, R., Chazette, P., Menut, L., and Bessagnet, B.: Aerosol chemical and optical properties over the Paris area within ESQUIF project, Atmos. Chem. Phys., 6, 3257–3280, doi:10.5194/acp-6-3257-2006, 2006.
Honoré, C. , Rouïl, L., Vautard, R., Beekmann, M., Bessagnet, B., Dufour, A., Elichegaray, C., Flaud, J.-M., Malherbe, L., Meleux, F., Menut, L., Martin, D., Peuch, A., Peuch, V. H., and Poisson, N.: Predictability of European air quality: The assessment of three years of operational forecasts and analyses by the PREV'AIR system, J. Geophys. Res., 113, D04301, doi:10.1029/2007JD008761, 2008.
Junker, C. and Liousse, C.: A global emission inventory of carbonaceous aerosol from historic records of fossil fuel and biofuel consumption for the period 1860–1997, Atmos. Chem. Phys., 8, 1195–1207, doi:10.5194/acp-8-1195-2008, 2008.
Kondo, Y., Miyazaki, Y., Takegawa, N., Miyakawa, T., Weber, R.J., Jimenez, J.L., Zhang, Q., and Worsnop, D.R., Oxygenated and water-soluble organic aerosols in Tokyo, J. Geophys. Res., 112, D01203, doi:10.1029/2006JD007056, 2007.
Konovalov, I. B., Beekmann, M., Richter, A., and Burrows, J. P.: Inverse modelling of the spatial distribution of NO_x emissions on a continental scale using satellite data, Atmos. Chem. Phys., 6, 1747–1770, doi:10.5194/acp-6-1747-2006, 2006.
Lattuati, M., Contribution à l'étude du bilan de l'ozone troposphérique à l'interface de l'Europe et de l'Atlantique Nord: Modélisation lagrangienne et mesures en altitude, Ph.D. Thesis, Univ. Pierre et Marie Curie, Paris, France, 1997.
Lonati, G., Ozgen, S., and Giugliano, M., Primary and secondary carbonaceous species in $PM_{2.5}$ samples in Milan (Italy), Atmos. Environ., 41, 4599–4610, 2007.
Madronich, S., McKenzie, R. E., Bjorn, L. O., and Caldwell, M. M., Changes in biologically active ultraviolet radiation reaching the earth's surface, J. Photochem. Photobiol., Biology, 46, 5–19, 1998.
Malm, W. C., Sisler, J. F., Huffman, D., Eldred, R. A., and Cahill, T. A.: Spatial and seasonal trends in particle concentration and optical extinction in the United States. J. Geophys. Res., 99, 1347–1370, 1994.

ACPD
10, 16861–16900, 2010

Malm, W. C., Day, D. E., and Kreidenweis, S. M.: Light scattering characteristics of aerosols as a function of relative humidity: part I – a comparison of measured scattering and aerosol concentrations using the theoretical models, J Air and Waste Manag. Assoc., 50, 686–700, 2000.

Nel, A.: Air pollution-related illness: Effects of particles, Science, 308, 804–806, 2005.

Nenes, A., Pilinis, C., and Pandis, S.: ISORROPIA: A new thermodynamic model for inorganic multicomponent atmospheric aerosols, Aquat. Geochem., 4, 123–152, 1998.

Offenberg, J. H. ,Lewandowski, M., Edney, E. O., Kleindienst, T. E., and Jaoui, M.: Investigation of a Systematic Offset in the Measurement of Organic Carbon with a Semicontinuous Analyzer, J. Air and Waste Manag. Assoc., 57(5), 596–599, 2007.

Patashnik, H. and Rupprecht, E. G., Continuous PM_{10} measurements using a tapered element oscillating microbalance, J. Air and Waste Manag. Assoc., 41, 1079–1083, 1991.

Peltier, R. E., Weber, R. J., and Sullivan, A. P.: Investigating a liquid-based method for online organic carbon dectection in atmospheric particles, Aer. Sci. Technol., 41, 1117–1127, 2007.

Pun, B., Seigneur, C., and Lohman, K.: Modeling secondary organic aerosol via multiphase partitioning with molecular data, Environ. Sci. Technol. 40, 4722–4731, 2006.

Ramanathan, V., Li, F., Ramana, M. V., et al.: Atmospheric brown clouds: Hemispherical and regional variations in long-range transport, absorption, and radiative forcing, J. Geophys. Res., 112, D22S21, doi:10.1029/2006JD008124, 2007.

Rolph, G. D.: Real-time Environmental Applications and Display sYstem (READY) Website (http://www.arl.noaa.gov/ready.php). NOAA Air Resources Laboratory, Silver Spring, MD, 2003.

Ruellan, S. and Cachier, H.: Characterisation of fresh particulate vehicular exhausts near a Paris high flow road, Atmos. Environ., 35, 453–468, 2001.

Sciare, J., Sarda-Estève, R., Favez, O., Cachier, H., Aymoz, G., and Laj, P.: Nighttime residential wood burning evidenced from an indirect method for calculating real-time concentration of particulate organic matter (POM), Atmos. Environ., 42, 2158–2172, 2008a.

Sciare, J., Oikonomou, K., Favez, O., Liakakou, E., Markaki, Z., Cachier, H., and Mihalopoulos, N.: Long-term measurements of carbonaceous aerosols in the Eastern Mediterranean: evidence of long-range transport of biomass burning, Atmos. Chem. Phys., 8, 5551–5563, doi:10.5194/acp-8-5551-2008, 2008b.

Sciare, J., Oikonomou, K., Cachier, H., Mihalopoulos, N., Andreae, M. O., Maenhaut, W., and Sarda-Estève, R.: Aerosol mass closure and reconstruction of the light scattering coefficient

ACPD
10, 16861–16900, 2010

over the Eastern Mediterranean Sea during the MINOS campaign, Atmos. Chem. Phys., 5, 2253–2265, doi:10.5194/acp-5-2253-2005, 2005.
Schmidt, H., Derognat, C., Vautard, R., and Beekmann, M.: A comparison of simulated and observed ozone mixing ratios for summer of 1998 in Western Europe, Atmos. Environ., 6277–6297, 2001.
Tsyro, S.: First estimates of the effect of aerosol dynamics in the calculation of PM_{10} and $PM_{2.5}$, EMEP Report (www.emep.int), 2002.
Turpin, B. J. and Huntzicker, J. J.: Secondary formation of organic aerosol in the Los Angeles basin: a descriptive analysis of organic and elemental carbon concentrations. Atmos. Environ., 25, 207–215, 1991.
Turpin, B. J. and Lim, H. J.: Species contributions to $PM_{2.5}$ mass concentrations: Revisiting common assumptions for estimating organic mass, Aer. Sci. and Technol., 35, 602–610, 2001.
Valari, M. and Menut, L.: Does increase in air quality models resolution bring surface ozone concentrations closer to reality?, J. Atmos. Ocean. Technol., 25(11), 1955–1968, doi:10.1175/2008JTECHA1123.1, 2008.
Vautard, R., Beekmann, M., Roux, J., and Gombert, D.: Validation of a hybrid forecasting system for the ozone concentrations over the Paris region, Atmos. Environ., 35, 2449–2461, 2001.
Verwer, J. G.: Gauss–Seidel Iteration for Stiff ODES from Chemical Kinetics, J. Sci. Comput., 15, 1243–1250, 1994.
Weber, R. J., Sullivan, A. P., Peltier, R. E., Russell, A., Yan, B., Zheng, M., de Gouw, J., Warneke, C., Brock, C., Holloway, J. S., Atlas, E. L., and Edgerton, E.: A study of secondary organic aerosol formation in the anthropogenic-influenced southeastern United States, J. Geophys. Res., 112, D13302, doi:10.1029/2007JD008408, 2007.
Wesely, M. L.: Use of variance techniques to measure dry air-surface exchange rates, boundary-layer meteorol., 44, 13–31, 1988.
Widory, D., Roy, S., Le Moullec, Y., Goupil, G., Cocherie, A., and Guerrot, C.: The origin of atmospheric particles in Paris: a view through carbon and lead isotopes, Atmos. Environ., 38, 953–961, 2004.
Zhang, Q., Worsnop, D. R., Canagaratna, M. R., and Jimenez, J. L.: Hydrocarbon-like and oxygenated organic aerosols in Pittsburgh: insights into sources and processes of organic aerosols, Atmos. Chem. Phys., 5, 3289–3311, doi:10.5194/acp-5-3289-2005, 2005.

ACPD
10, 16861–16900, 2010

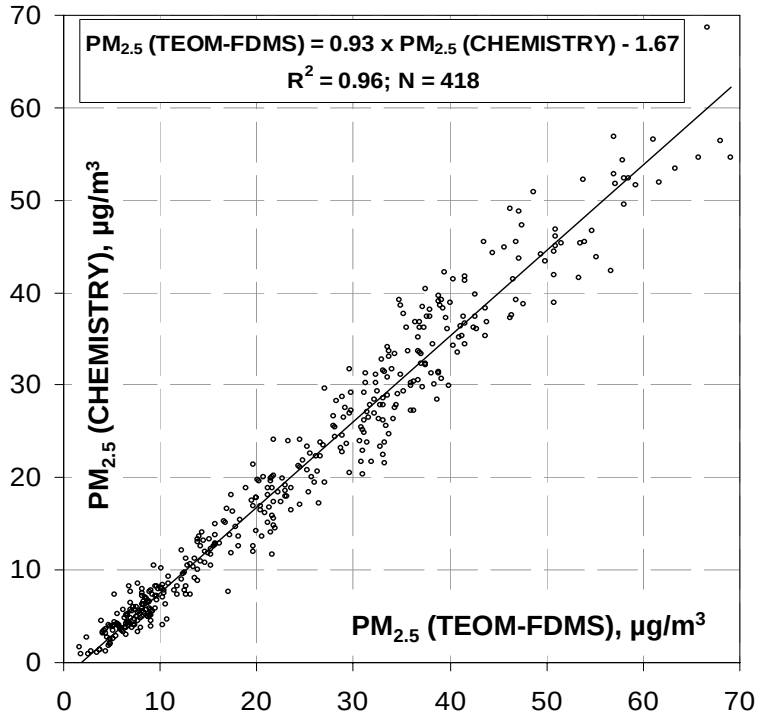

Fig. 1. Hourly $PM_{2.5}$ concentrations comparison between the TEOM-FDMS measurements and the reconstruction from the chemistry by summing EC, POM, and ions.

ACPD
10, 16861–16900, 2010

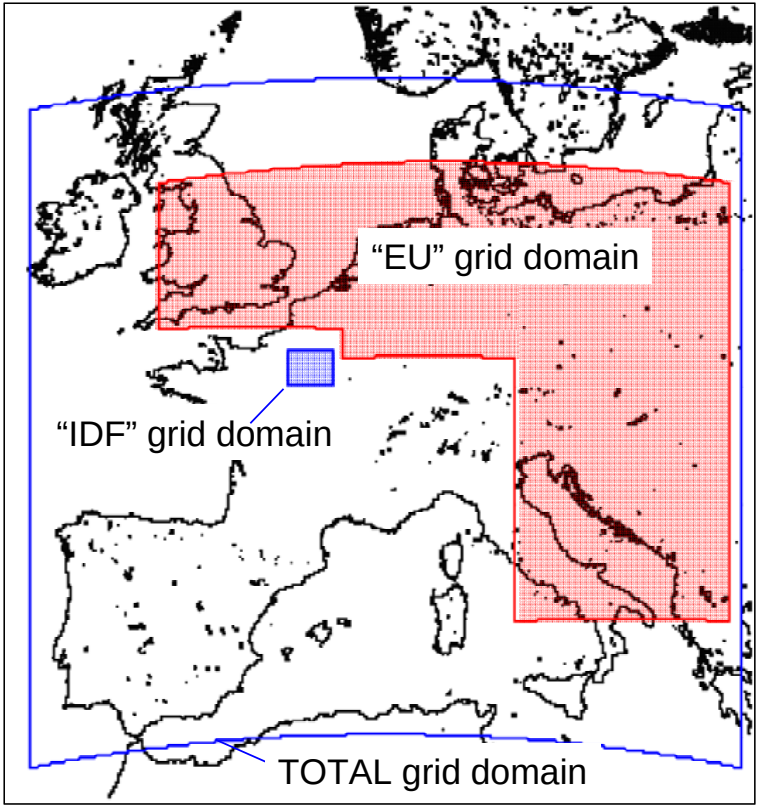

Fig. 2. Grid domain of the chemistry transport model CHIMERE. In blue the “IDF” domain comprising the Ile-de-France region surrounding Paris. In red the “EU” domain comprising part of North-Western and Central Europe.

ACPD
10, 16861–16900, 2010

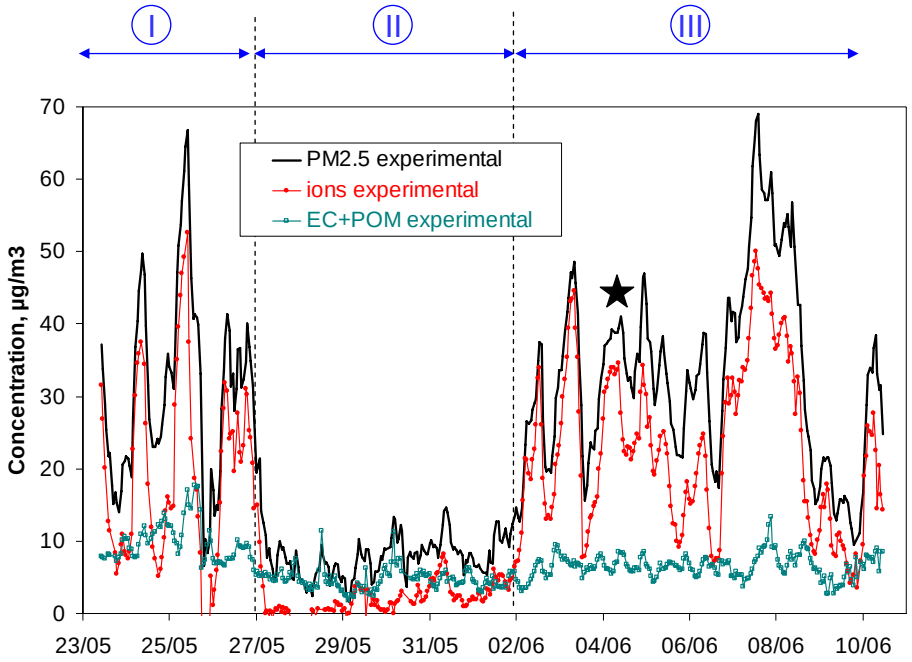

Fig. 3. Hourly $PM_{2.5}$ concentrations measured by TEOM-FDMS, fine carbonaceous aerosols (EC+POM) and reconstructed fine ions (ammonium nitrate+ammonium sulfate). Periods I and III stand for continental (European) air masses; period II stands for clean marine air masses. The black star corresponds to the pollution episode (plume case study) depicted in Sect. 5.1.

ACPD
10, 16861–16900, 2010

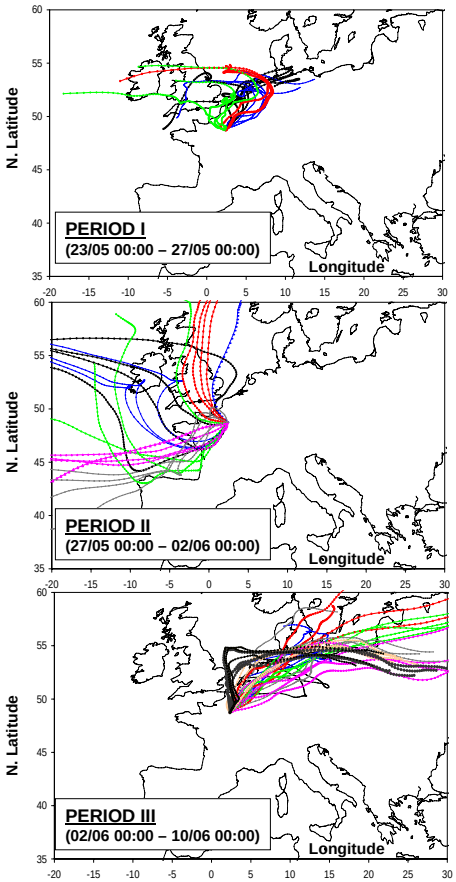

Fig. 4. 4-day backtrajectories ending at Paris (LHVP monitoring station; 500 m above ground level) and calculated every 6 h for period I **(a)**, period II **(b)**, and period III **(c)**.

ACPD
10, 16861–16900, 2010

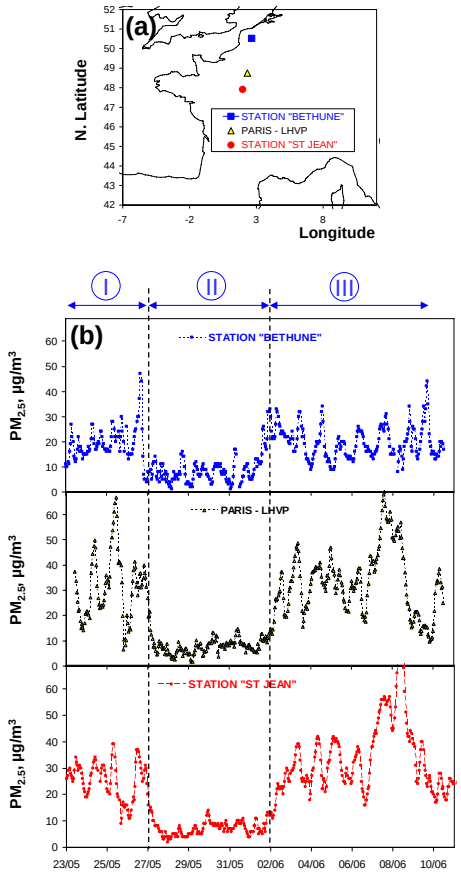

Fig. 5. Location of 3 ground stations with $PM_{2.5}$ (TEOM-FDMS) measurements **(a)** and temporal variation of $PM_{2.5}$ at these 3 stations **(b)**. Periods noted I, II, and III correspond to those reported in the text.

ACPD
10, 16861–16900, 2010

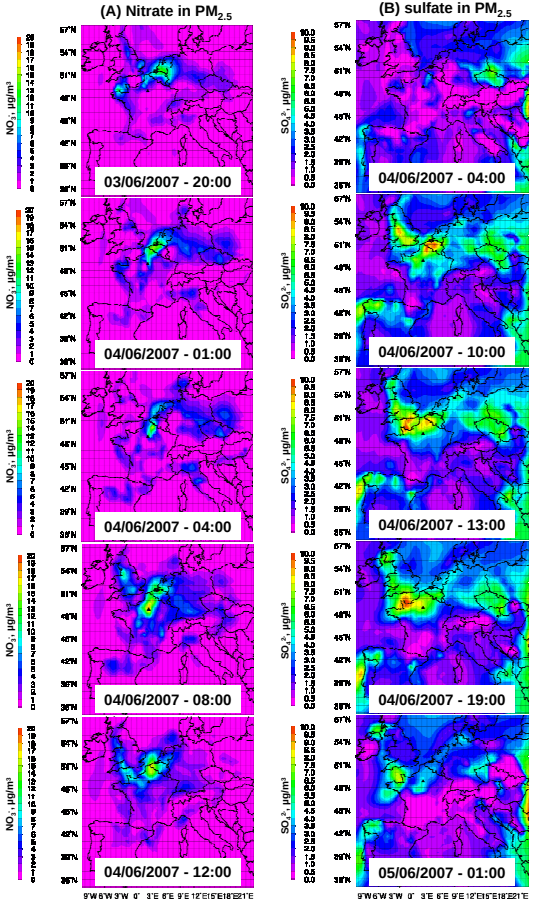

Fig. 6. Plume case study modeled by CHIMERE for fine nitrate **(a)** and fine sulfate **(b)** for the period 3–5 June 2007.

ACPD
10, 16861–16900, 2010

Contribution of regional versus continental emissions

J. Sciare et al.

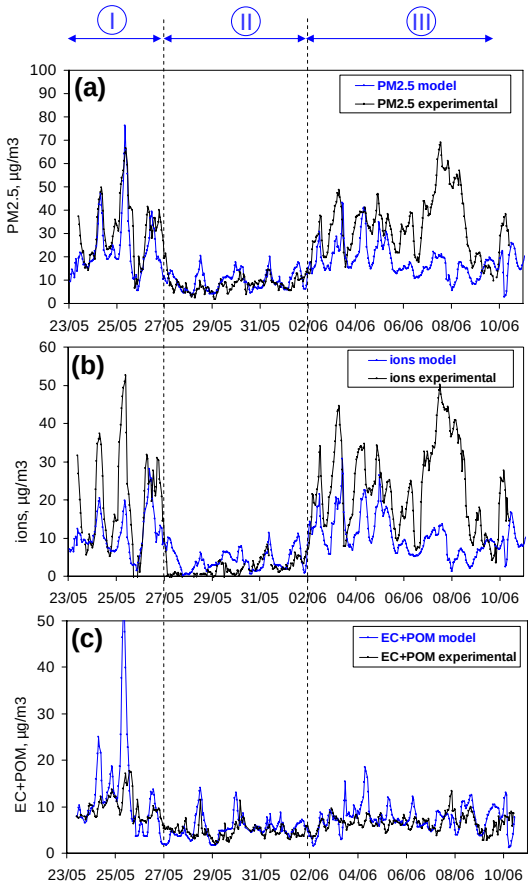

Fig. 7. Comparison between modeled and measured concentrations of $PM_{2.5}$ **(a)**, ion species (ammonium nitrate+ammonium sulfate) **(b)**, and carbonaceous matter (EC+POM) **(c)**. Periods noted I, II, and III correspond to those reported in the text.

ACPD
10, 16861–16900, 2010

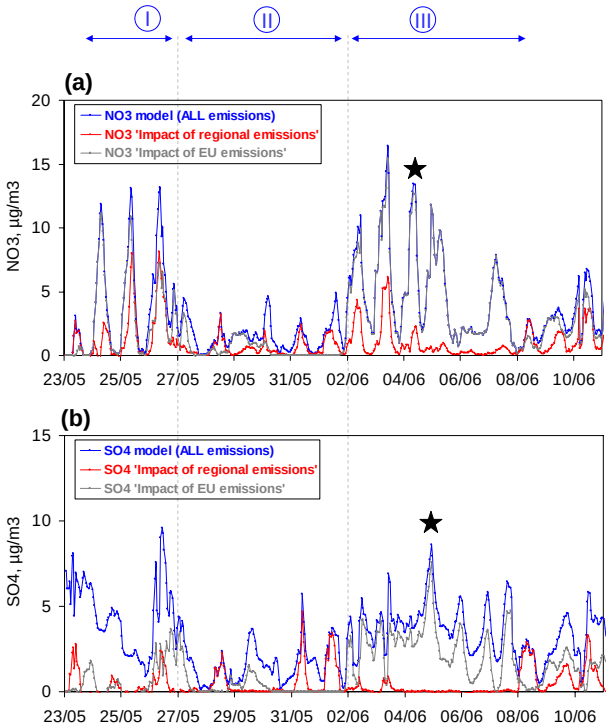

Fig. 8. Model scenarios for fine nitrate **(a)** and fine sulfate **(b)** for the base (reference) case (all emissions); the scenario without regional (IDF) emissions (in grey); and the scenario without European (EU) emissions (in red). The black star corresponds to the pollution episode (plume case study) depicted in Sect. 5.1.

ACPD
10, 16861–16900, 2010

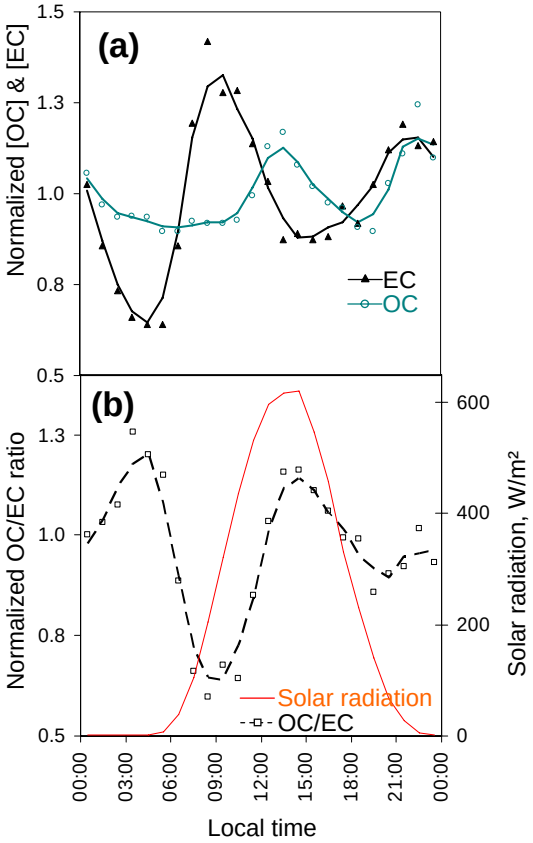

Fig. 9. (a) Diurnal variations of normalized concentrations of EC and OC. **(b)** Diurnal variation of normalized OC/EC ratio and solar radiation.

ACPD
10, 16861–16900, 2010

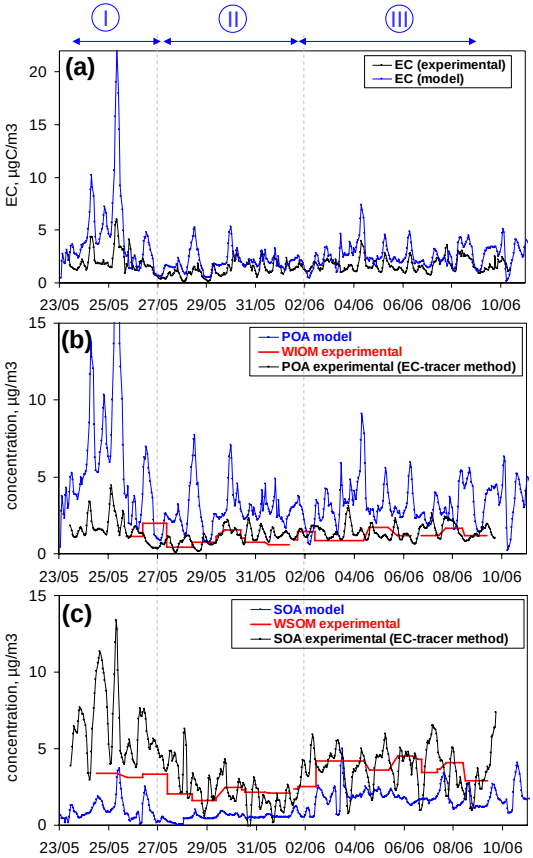

Fig. 10. Comparison of EC **(a)**, POA **(b)**, and SOA **(c)** from the CHIMERE model (in blue); the EC-tracer method determined by the OCEC Sunset Field instrument (in black); and WSOM and WSIOM determined from filter sampling (in red).

ACPD
10, 16861–16900, 2010